This article has been accepted for publication in a future issue of this journal, but has not been fully edited. Content may change prior to final publication. Citation information: DOI 10.1109/JSTARS.2021.3089151, IEEE Journal of Selected Topics in Applied Earth Observations and Remote Sensing

GA-SVR Algorithm for Improving Forest above Ground Biomass Estimation Using SAR Data

Yongjie Ji, Kunpeng Xu, Peng Zeng, Wangfei Zhang, *Member, IEEE*

***Abstract*—Synthetic aperture radar (SAR) features have been demonstrated that they have the potentiality to improve forest above ground biomass (AGB) estimation accuracy, especially including polarimetric information. Genetic algorithms (GAs) have been successfully implemented in optimal feature identification, while support vector regression (SVR) has great robustness in parameter estimation. The use of combined GAs and SVR can improve the accuracy of forest AGB estimation through simultaneously identifying the optimal SAR features and selecting the SVR model parameters. In this paper, 14 SAR polarimetric features were extracted from C-band and L-band full-polarization SAR images and worked as input SAR features, respectively. C-band data was acquired on GaoFen-3 mission, we also call it GF-3 image. L-band data was ALOS-2 PALSAR-2 data. Both feature subsets from GF-3 and ALOS-2 PALSAR-2 and SVR hyper parameters used in the forest AGB estimation were optimized by a GA processing, where 8 different settings of 3 kinds of parameters, as 512 kind of different combinations were applied for SVR hyper parameters searching field. The results of GA-SVR performance using the two datasets were presented and compared with two traditional methods: the algorithm of GA feature selection companied with default SVR parameters (GA +Default SVR), and the algorithm of GA feature selection companied with grid searching for SVR parameter selection (GA+Grid SVR). The results showed that the proposed GA-SVR algorithm improved the forest AGB estimation accuracy with cross-validation coefficient (CVC) of 80.21% for GF-3 and 71.41% for ALOS-2 PALSAR-2 data.**

***Index Terms*—Genetic algorithms (GAs), Forest above ground biomass (AGB), Support vector regression (SVR), Synthetic aperture radar (SAR)**

I. Introduction

FOREST above ground biomass (AGB) estimation plays an important role in research on global carbon cycle and climate change. Synthetic aperture radar (SAR) data, especially with polarimetric and interferometric information seems particularly useful for forest AGB estimation [1]. However, as the SAR data begins to mature and abundance, a large SAR feature sets can be generated, one key point for accurate forest biomass estimation using SAR data is to select the optimal discriminative features from the large feature sets, the other is to select the suitable retrieval models [2].By far, different methods including manual and automatic ways have been used to explore suitable SAR features and algorithms for forest AGB estimation [3-5]. The selected feature subsets combined with non-parametric-based algorithms like K-nearest neighbor (K-NN), random forest (RF) and support vector regress (SVR) showed better performance in forest AGB estimation [3,5].

SVR is the SVM implementation for regression and has the similar advantages of support vector machine (SVM). As the advantages including its structural risk minimization and leading to a convex quadratic programming problem during the training procedure, SVM algorithm always converges to the global solution for a given dataset regardless of initial conditions and has great ability to control overfitting problems and thereby good generalization [6, 7]. Therefore, SVR, taking the advantage of its ability to use small training sample data to produce relatively higher estimation accuracy than other approaches and to solve both linear and non-linear problems, becomes an important method to estimate forest AGB and other biophysical parameters using remote sensing data [3, 5, 8]. However, the impacts of forest AGB on scattering, attenuation, and emission of electromagnetic energy are complex and varying with forest horizontal and vertical structure and also the environment issues. Thanks for the abundance of SAR data and their special capability in measuring the structural and dielectric properties of the target, more and more features, which can response for different characterization of forest, were extracted from SAR data and applied in forest AGB estimation to improve the estimation accuracy. SVR, developed with the capacity of none linear fitting and used kernel trick to solve over-fitting problems in high-dimensional feature spaces, shows great potentiality in forest AGB estimation using abundant SAR features.

Despite the good performance shown by SVR, the robustness of SVR is limited by the suitable model parameters selection. Genetic algorithms (GAs) were reported to optimize the model parameters and feature selections in several previous studies. The results showed that GAs were capable of providing an efficient optimal feature subset and also the retrieval model parameters, respectively [9-11]. However, these studies did not address the synergy performance of selecting features and SVR model parameters simultaneously, like a GA-SVR algorithm proposed in this study, especially applied in the field of forest AGB estimation.

By far, GA-SVR algorithms have been widely employed in medical studies [12], traffic data analyses [13, 14], and

This work was supported by the National Natural Science Foundation of China (No.31860240) and Scientific Research Foundation of Education Department of Yunnan Province (No.2019J0182; 2020Y0393).
(Corresponding author: W. Zhang.)

Y. Ji, P. Zeng and W. Zhang are with the Forestry Collage, Southwest Forestry University, Kunming 650224, China (e-mail: mewhff@163.com).

K. Xu is with the Institute of Forest Resources Information Technique, Chinese Academy of Forestry, Beijing 100091, China (e-mail: xukp@ifrit.ac.cn).

industry studies [15]. However, most of the above-mentioned GA-SVR applications focused more on SVR model parameters optimization with GA but not considered identifying the optimal input feature subsets and the SVR model parameters simultaneously. Sukawattanavijit et al (2017) demonstrated the advantages of using GA-SVM algorithm in land-cover classification by performing the feature and SVM parameter optimization simultaneously. The results showed that the GA-SVM algorithm shows better performance on SVM parameter optimization and feature selection than the grid search algorithm. The average run time of GA-SVM is less than that of the grid search algorithm, the accuracy of classification using GA-SVM is also greater than that of the grid search algorithm [16]. SVM and SVR methods are used for different applications, the main aim of this study is to explore GA-SVR algorithm applied in forest AGB estimation with SAR data. Therefore, the study focusses on determining whether the GA-SVR algorithm, which optimize the input features and SVR model parameters simultaneously, can improve the accuracy of forest AGB estimation.

In section II, the theories of GA-SVR are introduced first. Then, in section III, the study area and datasets used in this paper are introduced. Methodologies of GA-SVR used for forest AGB estimation are presented in section IV. Results, discussion, and conclusions are shown and exposed in section V, VI, and VII respectively.

II. THEORY OF GA-SVR

A. Support vector regression

SVM, which was proposed by Vapnik in 1995, is a powerful and robust approach for information categorization and dataset classification. Its robustness includes the ability of structural risk minimization and the ability to solve both linear and nonlinear problems [14, 17]. The SVM classifier separates classes using an optimal hyperplane $w \cdot x + b = 0$, which maximize the margin between two groups. In order to achieve the maximum margin between the two classes, the largest margin is calculated with the summation of the shortest distance from the separating hyperplane to the nearest data point of both categories. The nearest data points are the so-called support vectors, which are also important features of the training samples. SVM using kernel trick maps input parameters into a high dimensional feature space to solve nonlinear problems. The nonlinear transformation defined by kernel function makes a linear classification in the new feature space (or the high dimensional feature space) equivalent to nonlinear classification in the original space (or the input space). Different kernel functions, such as linear functions, polynomial functions, sigmoid functions and radial basis functions (Radical Basis Function kernel, RBFs) have been widely used in SVM problems [18].

SVR, as an extension of SVM regression, is an approach to estimate a function that maps from input features to an unknown output based on training data. Similar to the SVM classifier, SVR has the same properties of the margin maximation and kernel trick for nonlinear problems. The SVR model is composed of a training model and a predicting model. At first, the training model is used to learn the relationship between input training fractional SAR polarimetric features and corresponding forest biomass, and then the learned relationship is applied in the predicting model of SVR to get the regression value for each inputted testing samples [17, 18].

Suppose the training set for regression is given as $\Omega=\{(x_1,y_1),(x_2,y_2),\cdots,(x_m,y_m)\}$, where x_i is the n-dimensional input feature vector, y_i is the corresponding output regression value for each x_i. Then the SVR approximates all pairs (x_i,y_i) while finds the minimum error or deviation, ε, and maps an input x_i to the target y_i by function $f(x)=w\cdot x+b$. That is, for every input vector x_i in Ω, $w\cdot x_i+b-y_i\le\varepsilon$ and the margin is $margin=\frac{1}{\|w\|}$. In regression problems, ε is the difference between estimated values and real values, w is known as the weight vector and b is the bias. The SVR training becomes a constrained optimization problem by minimizing $\|w\|^2$ to maximize the margin. With allowing some errors to deal with noise in the training data, the slack variables ξ_i and ξ_i^* are introduced in the constrained optimization problem, that is,

$$\text{Minimize: } \frac{1}{2}\|w\|^2+C\sum_{i=1}^{n}(\xi_i+\xi_i^*) \quad C>0,$$

$$\text{Subject to: } \begin{cases} y_i-w\cdot x_i-b\le\varepsilon+\xi_i & \forall(x_i,y_i)\in\Omega \\ w\cdot x_i+b-y_i\le\varepsilon+\xi_i^* & \forall(x_i,y_i)\in\Omega \\ \xi_i,\xi_i^*\ge 0 & (i=1,2,\cdots,n) \end{cases} \quad (1)$$

The constant C is the trade-off parameter which determines the trade-off between the weight factor and approximation error. ξ_i and ξ_i^* impose a penalty on excess deviation larger than ε to deal with the infeasible constrains of the optimization problem.

The optimization problem can be solved by construct a Lagrange function by introducing Lagrange multipliers and then transformed a dual optimization problem, that is,

$$\text{Maximize: } \begin{aligned} L(\alpha_i,\alpha_i^*) &= \sum_{i=1}^{n}y_i(\alpha_i-\alpha_i^*)-\varepsilon\sum_{i=1}^{n}(\alpha_i+\alpha_i^*) \\ &-\frac{1}{2}\sum_{i=1}^{n}\sum_{j=1}^{n}(\alpha_i-\alpha_i^*)(\alpha_j-\alpha_j^*)x_i x_j \end{aligned}$$

$$\text{Subject to: } \begin{cases} \sum_{i=1}^{n}(\alpha_i-\alpha_i^*)=0 \\ 0\le\alpha_i,\alpha_i^*\le C \end{cases} \quad (2)$$

where α_i and α_i^* are Lagrange multipliers and $L(\alpha_i,\alpha_i^*)$ represents the Lagrange function.

After we solved the dual optimization problems, the linear SVR function $f(x)$ becomes the following function,

$$f(x)=\sum_{i=1}^{n}(\alpha_i-\alpha_i^*)x_i x+b \quad (3)$$

Where $(\alpha_i-\alpha_i^*)\ne 0$, α_i and α_i^* are support vectors and n is the number of support vectors.

This article has been accepted for publication in a future issue of this journal, but has not been fully edited. Content may change prior to final publication. Citation information: DOI 10.1109/JSTARS.2021.3089151, IEEE Journal of Selected Topics in Applied Earth Observations and Remote Sensing

For non-linear regression, the same kernel trick in SVM can be applied by replacing the inner product of two vectors x_i , x_j with a kernel function $K\left(x_i,x_j\right)$. Then the non-linear problem can be solved as a linear regression. That is,

$$L\left(\alpha_i,\alpha_i^*\right)=\sum_{i=1}^{n}y_i\left(\alpha_i-\alpha_i^*\right)-\varepsilon\sum_{i=1}^{n}\left(\alpha_i+\alpha_i^*\right) -\frac{1}{2}\sum_{i=1}^{n}\sum_{j=1}^{n}\left(\alpha_i-\alpha_i^*\right)\left(\alpha_j-\alpha_j^*\right)K\left(x_i,x_j\right)$$

$$\text{Subject to: }\begin{cases}\sum_{i=1}^{n}\left(\alpha_i-\alpha_i^*\right)=0\\ 0\le\alpha_i,\alpha_i^*\le C\end{cases}\qquad(4)$$

The non-linear SVR function $f\left(x\right)$ becomes the following function,

$$f\left(x\right)=\sum_{i=1}^{n}\left(\alpha_i-\alpha_i^*\right)K\left(x_ix\right)+b\qquad(5)$$

Since RBF kernel has been widely used in different studies and performs better in problems that there is no prior knowledge, in this paper, RBF defined by x_i and x_j is used in the GA-SVR models. It is defined as:

$$K\left(x_i,x_j\right)=\exp(-\gamma\cdot\left\|x_i,x_j\right\|^2)\qquad(6)$$

where γ is the parameter set the width of the Gassian kernel.

B. Genetic algorithm

GAs, which are adapted from the Darwinian principle of natural selection, have been successfully used in generating global solutions for optimization problems. They are inspired by the biological evolution process that survival of the fittest resulting from natural genetic variation [13, 16]. Such variation includes selection, crossover and mutation. The selection operator is used for next generation parents selecting. Part of the previous generated population is selected according to an elitism percentage and works as parents for the next generation. In this procedure, most fitted members survive while the least fitted members are eliminated. Several selection operators such as random uniform, roulette wheel and tournament are available in GAs for selection operation. Crossover operator inspired by DNA strand crossover in biological organism reproduction combines two parents to create new generation from current population. The crossover operator can be performed by using a strategy like single-point crossover, multi-points crossover, or homologous crossover. The mutation operator maintains the diversity of the population and avoids local optimal solution by randomly changes a parent to create new children.

The process of GAs is described as follows: first, the initial population is generated. Each individual member in the generated population is defined by a chromosome consisted by a set of binary bits representing the selected input features and the model parameters. Each chromosome is represented by a binary-coded one-dimensional array. Then the fitness function of each chromosome is evaluated based on SVR model cross-validation using certain features subset and hyper parameters setting that the chromosome represents as. Next, the evolutionary process of selection, cross-over, and mutation is implemented to evolve towards better solutions by creating the new generation. New generation is then used for further iteration. Finally, when the maximum number of generations or a minimum threshold is reached the GAs process stops and the best configuration for the estimation model is outputted.

C. GA-SVR model

Fig.1 represents the flowchart of GA-SVR for forest biomass estimation procedure with GF-3 and ALOS-2 PALSAR-2 polarimetric Data.

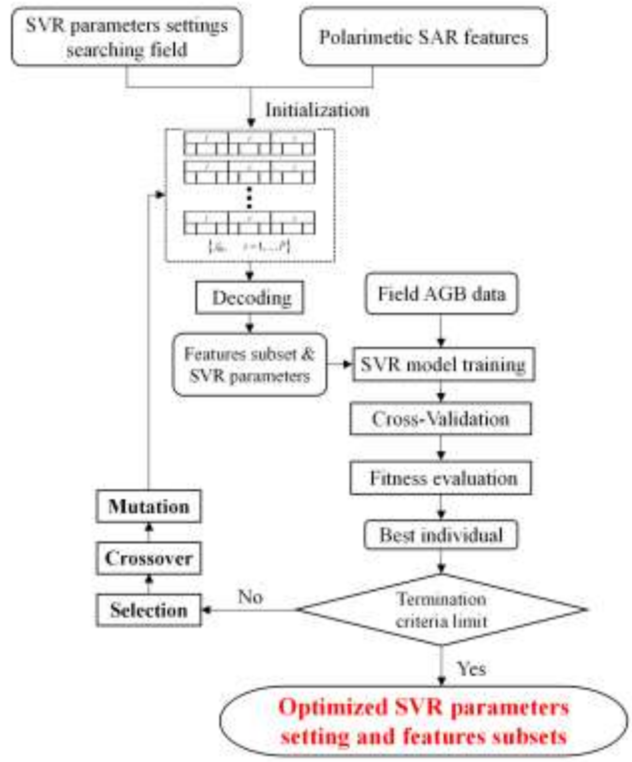

Fig.1. The flowchart of GA-SVR algorithm

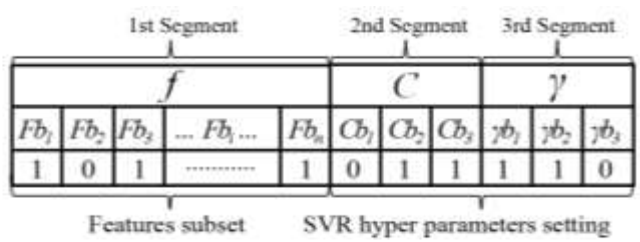

Fig.2. Design of the chromosome for GA-SVR.

The GA-based optimization is used to find the best input feature and SVR parameter values. Thus, the chromosome of the GA contained a set of bits (Fig.2) [15, 16]. The first part "Feature Selection" or 1st segment of chromosome represents the particular input features selected. This part includes *f* bits, which equals to the number of original features set. In this paper, original feature set is the features extracted from the SAR image by polarimetric decomposition algorithms. The second part "SVR settings" or the last two segments represent two SVR parameters like the trade-off parameter C , and the γ of the width of the RBF kernel. In Fig.2, Fb_1~Fb_n represent the

This article has been accepted for publication in a future issue of this journal, but has not been fully edited. Content may change prior to final publication. Citation information: DOI 10.1109/JSTARS.2021.3089151, IEEE Journal of Selected Topics in Applied Earth Observations and Remote Sensing

input features, when Fb_i = 1, then corresponding feature is selected. Otherwise, Fb_i = 0, which means the feature is not selected. n is the number of bits representing the input features. $Cb_1 \sim Cb_3$ is the binary code that indexes the value of C *and* $\gamma b_1 \sim \gamma b_3$ is the binary code that indexes the value of γ, Table.1 details the searching range of two SVR parameters.

TABLE I
SEARCHING RANGE OF SVR PARAMETERS

Hyperparameter	Values
C	50, 100, 150, 200, 500, 1000, 1500, 2000
γ	0.01, 0.02, 0.05, 0.1, 0.15, 0.2, 0.5, 1.0

λ_g^i is the i chromosome of the g generation, P is the number of individuals, G is the number of generations. As the chromosomes are designed, the population size is set by the user and then the initial population is generated. In Fig.1, the chromosomes are $\{\lambda_0^i, \quad i=1,...,P\}$, where λ_0^i is the i chromosome of the first generation.

After generating of the initial population, a typical SVR process is performed by using the assigned parameter values and input training data-set. The performance of each solution is validated by the fitness function. In this letter, we define the fitness function with a m repeated K-fold cross validation (K-CV) method. The fitness function is shown in (7)[15]

$$\text{Fitness} = (1 - \frac{\sum_{i=1}^{K\times m} error}{K\times m}/AGB_{mean})*100 \qquad (7)$$

where *error* depicts roots mean squared error at each procedure, K is the number of folds, and m is the number of repetitions and AGB_{mean} is mean value of the field measured forest AGB.

Then the individual with highest fitness is recorded and if the termination criterion is satisfied, the optimal values of input features and SVR parameters are the GA-SVR output. If the termination criterion is not satisfied, the evolution procedure including selection, crossover and mutation are applied for the next generation until the termination criterion is satisfied. Since the average fitness of the population will increase each evolution cycle, the desired results are obtained with the iteration.

III. STUDY AREA, SAR DATA AND FIELD DATA

A. *Study Area*

The study area, approximately 44 km^2 in size, is located in the Yunnan province of southwest of China. The work was carried out at the Xiaoshao timberland in Yiliang county (24° 04′ to 24° 39′ N, 103° 02′ to 103° 12′ E, Fig.3). The topography ranges from 1300 to 2500 m. The slopes varies between 0～30° . The climate type is a Subtropical Monsoon Climate. The annual mean temperate is around16.3℃. The average annual precipitation is around 898.9 millimeters. The dominated tree species include *Pinus yunnanensis* and *Pinus armandii Franc*h. The average height ranges from 5m～20m, the average biomass value is around 60 Mg/ha and the maximum biomass here is no more than 200 Mg/ha.

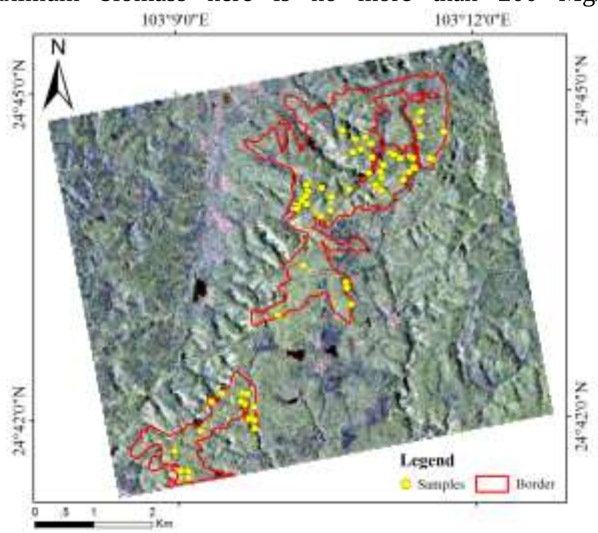

Fig.3.The test site at Xiaoshao timberland in Yiliang county, Yunnan province, China. The yellow points show the location of the collected samples, the red line shows the boundary of the samples distribution. The background is a Pauli RGB image of GF-3, acquired on May 18, 2018.

B. *Aboveground Biomass Data*

68 forest plots were surveyed in 2019 with the angle count method. At each sampling plot, all trees with a diameter at the breast height (DBH at 1.3 m height) great than or equal to 5 m were measured. The height, tree species, number of stems and DBH of these trees within the limited plot radius were gathered. The location of each sampling plot was located using a differential GPS (global position system) equipped with Leica Viva GS14-GNSS antenna base-station and CS15 receiver. The AGB was calculated for 1 ha using equation (8) developed by Huang et al [19].

$$w = av^b \qquad (8)$$

where w (in Mg/ha) is the biomass, a is the scaling factor between allometric exponent b and the stem volume and v. For *Pinus yunnanensis* $a = 0.8569$, $b = 0.8564$.

The stem volume v was calculated by equation (9) according to [20].

$$v = F_g \sum_{i=1}^{k} Z_i \bullet (fh)_i \qquad (fh)_i = V_i / g_i \qquad (9)$$

where F_g is the basal area factor, in this study, $F_g = 1$. k is the number of diameter class at each measured sampling plot. Z_i is the number of trees at diameter class of i. $(fh)_i$ is the Form-height at diameter class of i, it is calculated by the stem volume V_i checked in the Single Volume Table and the basal area g_i at diameter class of i.

All the measured samples are located in the study area and are shown in Fig.3 as yellow points. In this study, the samples were averaged with biomass difference no more than 3 Mg/ha to reduce the random effects resulted from forest structure or terrain effects. The samples with different biomass values are shown in Table 2.

This article has been accepted for publication in a future issue of this journal, but has not been fully edited. Content may change prior to final publication. Citation information: DOI 10.1109/JSTARS.2021.3089151, IEEE Journal of Selected Topics in Applied Earth Observations and Remote Sensing

TABLE II
FOREST BIOMASS DISTRIBUTION OF THE SAMPLES

No	Values(Mg/ha)	No	Values(Mg/ha)	No	Values(Mg/ha)
1	9.34	11	38.08	21	67.2
2	13.67	12	40.28	22	76.36
3	15.94	13	42.52	23	82.4
4	18.87	14	46.36	24	86.18
5	21.87	15	49.27	25	91.06
6	25.54	16	52.54	26	95.22
7	28.80	17	54.57	27	106.47
8	31.66	18	58.95	28	119.32
9	35.18	19	61.02	29	121.68
10	9.34	20	63.55	30	131.17

C. SAR Data

A scene of GF-3 (Fig.4 a) and a scene of ALOS-2 PALSAR-2 (Fig.4 b) full-polarimetric images were collected to analyze the performance of proposed method in forest AGB estimation. Table.3 lists the detail information of the two investigated SAR images.

TABLE III
DETAIL INFORMATION OF THE ACQUIRED GF-3 DATA

Parameters	GF-3	ALOS-2 PALSAR-2
Collected Date	2018-05-18	2016-04-02
Polarization	HH, HV, VH, VV	HH, HV, VH, VV
Wavelength	5.55cm	24.25cm
Incidence Angle	39.104°	33.865°
Range pixel spacing	2.248 m	2.86m
Azimuth pixel spacing	5.120 m	3.21m
Orbit direction	Ascending	Ascending
Observation Mode	Full-pol stripmap	High sensitive
Swath (km)	30	40

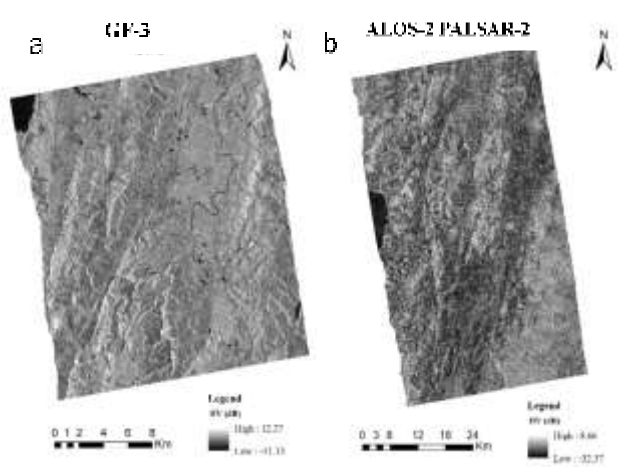

Fig.4.The acquired GF-3 and ALOS-2 PALSAR-2 images in the test site. The geocoded HV channel is showed here as an example for both of them, respectively.

IV. METHODOLOGY

A. SAR data preprocessing

The preprocessing of GF-3 and ALOS-2 PALSAR-2 data includes radiometric calibration, geo-referencing and speckle reduction. The radiometric calibration consists of converting digital numbers to backscatter coefficient in the four polarizations, and was done on the basis of following equations. (10) is for GF-3 and (11) is for ALOS-2 PALSAR-2.

$$\sigma^0_{dB} = 10\log_{10}\left(P^I * \left(QualifyValue/32767\right)^2\right) - K_{dB} \quad (10)$$

where $P^I = I^2 + Q^2$, I and Q are real in-phase component and the imaginary quadrature component, respectively. $QualifyValue$ is the maximum value of the scene image before its quantification. K_{dB} is the calibration constant for GF-3 products, it varied with different product type, here its value is -19dB, the information for GF-3 calibration comes from GF-3 user handbook.

$$\sigma^0_{dB} = 10\log_{10}\left(I^2 + Q^2\right) + CF \quad (11)$$

where I and Q are real in-phase component and the imaginary quadrature component, respectively. CF is the calibration coefficient factor for ALOS-2 PALSAR-2 data, $CF = -83dB \pm 0.406dB$ [21].

GF-3 and ALOS-2 PALSAR-2 data were read and calibrated using an interactive data language (IDL) application, then the decomposition parameters and backscattering intensity features were achieved by IDL script through transferring functions in PolSARpro 4.2, finally these feature channels were geo-coded also by IDL script through transferring functions from radar software. In this procedure, a 5×5 refined Lee filter was applied to the GF-3 and ALOS-2 PALSAR-2 data to reduce speckle noise.

B. SAR polarimetric processing and polarimetric features extraction

At the forest covered areas, we often assume the reciprocity theorem holds (the backscatter from HV = the backscatter from VH), especially when higher frequency (X- or C-band) images are used in remote sensing radar imaging for forest inventory. However, for lower frequencies, we should consider the Faraday rotation which destroyed the reciprocity assumption. To reduce the reciprocity phenomenon effects, in this study, we extracted polarimetric decomposition parameters not only from Freeman-Durden decomposition, but also from Yamaguchi decomposition, because Freeman-Durden decomposition algorithm assumes reciprocity theorem holds, while the Yamaguchi decomposition deals with the non-reciprocity scattering cases.

In this paper, we selected linear backscatter intensity features like HH, HV, VH and VV as four basic polarimetric features. Except them, 10 polarimetric decomposition features were extracted using 3 polarimetric decomposition methods. The selected polarimetric decomposition methods include above mentioned Freeman-Durden, Yamaguchi algorithms and also the popular used Cloude-Pottier decomposition method [22]. Among them, Freeman-Durden and Yamaguchi methods are model-based decomposition methods, they model the covariance matrix as the contribution of several scattering mechanisms. For Freeman-Durden method, three scattering mechanisms, such as surface, double bounce and volume are extracted from the covariance matrix and work as three features in this study. Yamaguchi et al added a Helix scattering

This article has been accepted for publication in a future issue of this journal, but has not been fully edited. Content may change prior to final publication. Citation information: DOI 10.1109/JSTARS.2021.3089151, IEEE Journal of Selected Topics in Applied Earth Observations and Remote Sensing

mechanism as the fourth component to develop the Freeman-Durden decomposition algorithm. Cloude-Pottier decomposition is an Eigenvector-Eigenvalue based decomposition method, it uses eigenvalues and eigenvectors of the coherency to compute entropy (H), which indicates the degree of scattering mechanisms randomness, Alpha angle (α), which measures the average or dominant scattering mechanisms, and anisotropy (A), describes the intensity disparity between the second and the third scattering mechanisms. For the theory details of target decomposition method mentioned here, the readers are referred to literatures [23-26].

In this study, a total of 14 polarimetric SAR parameters were extracted from GF-3 and ALOS-2 PALSAR-2 images respectively. Parameters generated from four linear backscatter intensities were named as HH, HV, VH, and VV, they measure the backscattering power of the scattering object from each channel. In this study, the parameters coming from Freeman-Durden decomposition were defined as F-Vol, F-Dbl and F-Odd. The parameters extracted from Yamaguchi decomposition were defined as Y-Vol, Y-Dbl, Y-Odd, and Y-Hlx. F-Vol and Y-Vol describe the scattering mechanism of vegetation scatter from randomly oriented dipoles. F-Dbl and Y-Dbl measure scattering mechanism like dihedral corner reflector. F-Odd and Y-Odd depict scattering mechanism similar with first-order Bragg surface scattering. Y-Hlx detects scattering mechanism from complicated man-made objects. The parameters calculated from Cloude-Pottier decomposition were defined as Entropy-H, Anisotropy, and Alpha. Entropy-H indicates the level of randomness found from each target, Anisotropy measures the amount of mixing between the second and third scattering mechanisms, Alpha describes the scattering source for a given scattering mechanism described by an eigenvector [27]. For the parameters measuring the power of scattering, we kept both their descriptions with power state and their transformation into dBs and named their dB forms with their original name adding '-dB'.

C. Feature selection and SVR parameter optimization Using GA-SVR algorithm

The proposed GA-SVR algorithm was executed in the PYTHON 2.7 development environment. GA and SVR have separate roles in the forest biomass estimation procedure by the proposed GA-SVR algorithm. The SVR is trained by input training data-set and predicted forest AGB, while GA is used to optimize SVR to the best prediction based on SVR accuracy. It leads SVR to the best prediction by selecting optimal input feature subset and finding optimal SVR parameters. The main steps of proposed GA-SVR are as follows.

Step1. Create the training samples and validation samples: The training samples and validation samples were collected during field work. Then their related 14 features were extracted using PolSARpro program. In this study, 30 samples were used for the both training and validation samples, 15 folds cross validation were used to avoid the over-fitting.

Step2. The procedure of GA-SVR algorithm performance: it included the design of chromosome, the calculation of the fitness function and inputting of the SAR parameters. The chromosomes descried in Fig.2 are coded in binary form. The first 14 bits record feature combination, the bit with value of 1 means the corresponding feature is selected, while the value is 0, it means that the feature is not selected. The last 6 bits store the SVR parameters, the first three bits depict eight different values of C in binary code, the followed three bits represent the eight different values of γ in binary code. To improve the efficiency of the algorithm, we set the value of ε as 1 according to previous studies [8, 11, 28]. In this paper, K=15 and m=1 were applied for the fitness function. Other parameters were set as follows: tournament selection, initial population number = 35; number of generations = 200; crossover rate = 0.9 with single-point crossover; mutation rate = 0.1 with random mutation.

Step3. Run the SVR algorithm for forest AGB estimation. Based on the optimized features subset and SVR parameters of GA, the forest biomass values were calculated using the SVR model. For further analysis, the forest biomass estimation results of GA-based feature selection with default SVR parameters and the results of SVR parameters optimized with traditional grid search method after GA-based feature selection were compared with the results obtained using the proposed GA-SVR algorithm. Their performances were assessed by evaluating the scatter plots between the predicted and observed results. Determination coefficient (R^2) and cross-validation coefficient (CVC) were used as the parameters to evaluate the estimation accuracy. The two parameters are respectively expressed as:

$$R^2 = \frac{\sum_{i=1}^{n}\left(y_i - \bar{y}\right)^2}{\left(y_i - \bar{y}\right)^2} \tag{12}$$

where y_i is the estimation result, y_i is the observation result, $\bar{y}$ is the observation mean value and n is the sample numbers.

$$\text{CVC} = 1 - \frac{\sum_{i=1}^{K\times m} error}{K\times m} * 100\% \tag{13}$$

The roots mean square error (RMSE) is also used in this study to describe the accuracy.

V. Results

In this paper, as the main objective focusses on identifying the feasibility of proposed GA-SVR algorithm for forest AGB estimation. We present the comparison of the forest biomass estimation results using three methods including the proposed GA-SVR algorithm, the algorithm of GA feature selection combined with default SVR parameters (GA + Default SVR), and the algorithm of GA feature selection combined with grid searching for SVR parameter selection (GA+Grid SVR). To present the difference of the above mentioned three algorithms, we distinguished the steps of the three algorithms in table IV when preforming the procedure of forest AGB estimation. Then the performances of these algorithms on GF-3 and ALOS-2 PALSAR-2 data were both provided here as follows.

TABLE IV
THE DIFFERENCE OF GA-SVR, GA+DEFAULT SVR, AND GA+GRID SVR ALGORITHMS

Methods	Feature selection	Model parameter selection	Model
GA-SVR	Combination optimization	Combination optimization	SVR
GA+Default SVR	GA optimization	Default	SVR
GA+Grid SVR	Using the results of *Default SVR+GA*	Grid searching	SVR

A. GF-3 data

The performance of the proposed GA-SVR algorithm in the forest AGB estimation was analyzed and compared with the results of GA+Default SVR and GA+Grid SVR. Their performance was assessed by evaluating the scatter plots between the observed and predicted results. The features and model parameter selected in the procedure were also showed here for reference. Optimal selected features and the selected values for SVR model parameters were provided in Table V.

TABLE V
PARAMETERS AND FEATURE OPTIMIZATION FOR GF-3 OF GA-SVR, GA+DEFAULT SVR AND GA+GRID SVR

Methods	C	γ	Selected feature	Count
GA-SVR	500	0.15	Y_Vol; F_Vol; F_Dbl; Entropy; F_Dbl_db; F_Odd_db	6
GA+ Default SVR	100	default	Y_Vol; Y_Hlx; F_Odd; F_Dbl; Alpha; F_Dbl_db;F_Odd_db; Y_Hlx_db; Y_Odd_db	9
GA+ Grid SVR	500	0.05	Y_Vol; Y_Hlx; F_Odd; F_Dbl; Alpha; F_Dbl_db;F_Odd_db; Y_Hlx_db; Y_Odd_db	9

The optimized SVR parameters (C AND γ) of GA-SVR algorithm were 500 and 0.15, respectively, for the Default SVR+GA algorithm, the default value for C was 100, and the default value for γ was calculated by 1 dividing the numbers of input features, for the GA+Grid SVR algorithm, the values were 500 and 0.05, respectively. Since we aimed to compare the optimization difference between features and model parameters optimization separately and features and model parameters optimization simultaneously, the selected features for GA+Default SVR and GA+Grid SVR are totally same. However, the difference of the selected feature combination of GA-SVR and the other two algorithms was obvious. It used less selected features, 6 here and 9 compared with other two algorithms. To evaluate the accuracy and also the capability of each model to predict forest AGB, there was a comparison between observed and predicted values that was shown in Fig.5. In Fig.5, we also presented the iterative procedure of GA feature selection or Grid model parameter searching. Agreement lines (1:1 lines) were shown in Fig.5 a1, b1, and c1 in which observed and predicted forest AGB are equal.

Fig.5 a1 shows scattered plots of observed and predicted forest AGB using GA-SVR model. It is clear from Fig.5 a1 that GA-SVR performs better in low forest AGB than high ones. Fig.5 a2 shows that scattered plot of observed and predicted forest AGB by GA+Default SVR. For both low and high forest AGB level, GA+Default SVR performance was decreased. The scatter plot of observed and predicted forest AGB using GA+Grid SVR is shown in Fig.5 c1. As it can be seen from Fig.5 c1, the performance seems to be better than the GA+Default SVR algorithm in prediction of high forest AGB, but worse than the GA-SVR algorithm in prediction of low forest AGB. Fig.5 a2 shows that GA is stable at generation 100 after 8 times iteration of each best individuals. The fitness also improved from 70% to 80%. The phenomenon confirmed the effectiveness of searching and convergence. Fig.5 b2 shows the lowest accuracy with value around 73% while Fig.5 c2 shows the better accuracy with value of 76.88%. Fig.5 a2, b2, and c2 revealed the importance of feature and model parameter optimization procedure, it also confirmed the necessity of optimizing input features and estimation model parameters simultaneously.

Statistical parameters of the three algorithms established with GF-3 are given in table VI.

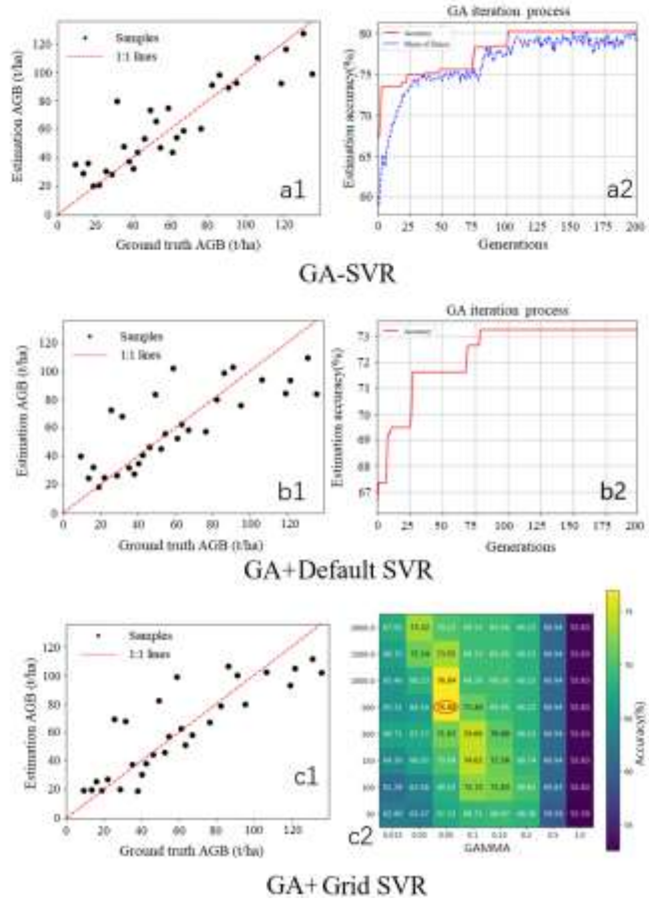

Fig.5. Biomass estimation results vs ground truth data (Results from GF-3). (a1) Iterative procedure of GA feature selection for GA-SVR algorithm; (a2) GA-SVR estimation results; (b1) GA iteration procedure for GA+Default SVR algorithm; (b2) GA+Default SVR estimation results; (c1) Grid model parameter searching procedure for GA+Grid SVR; (c1) GA+Grid SVR estimation results.

This article has been accepted for publication in a future issue of this journal, but has not been fully edited. Content may change prior to final publication. Citation information: DOI 10.1109/JSTARS.2021.3089151, IEEE Journal of Selected Topics in Applied Earth Observations and Remote Sensing

TABLE VI
(GF-3) RESULTS COMPARISON BETWEEN GA-SVR, GA+DEFAULT SVR AND GA+GRID SVR

Methods	CVC (%)	RMSE (Mg/ha)	R^2
GA-SVR	80.21	12.01	0.79
GA+Default SVR	73.25	16.24	0.62
GA+Grid SVR	76.88	14.03	0.73

Result comparison of three algorithms also reveals the superiority of GA-SVR algorithm over the other two algorithms. Using GA-SVR algorithm improves prediction accuracy about 10% compared with GA+Default SVR. Processing feature and model parameter optimization step by step, GA+Grid SVR has inferior estimation accuracy than GA-SVR. The R^2 is 0.73 and the CVC value is 76.88%. Without model optimization, the results of GA+Default SVR showed worst results with R^2 = 0.73 and CVC = 73.25

B. ALOS-2 PALSAR-2 data

The numerical results for the performance of above mentioned three algorithms applied on ALOS-2 PALSAR-2 data are shown in Table VII. The table shows the optimized SVR parameter sets and the selected input polarimetric features for ALOS-2 PALSAR-2 using GA-SVR, GA+Default SVR, and GA+Grid SVR. The optimized SVR parameters (C and γ) for GA-SVR algorithm were 1500 and 0.02, respectively. Compared with GF-3, the C value is higher while the γ value is lower. It reveals the lower speed of GA-SVR algorithm in forest AGB estimation. The selected polarimetric features are also different with the features selected for GF-3 data. It means the different optimization feature combination during the forest AGB estimation procedure. For the GA + Default SVR algorithm and the GA+Grid SVR algorithm, the selected features are less that selected for GF-3 data. Here only 5 polarimetric input features are selected to get best performance.

TABLE VII
PARAMETERS AND FEATURE OPTIMIZATION FOR ALOS-2 PALSAR-2 OF GA-SVR, GA+DEFAULT SVR AND GA+GRID SVR

Methods	C	γ	Selected feature	Count
GA-SVR	1500	0.02	Y_Vol; Y_Odd; Y_Hlx; F_Odd; HV_dB; VH_dB; Y_Odd_db; Anisotropy	8
GA+ Default SVR	100	default	Yam_Hlx; Anisotropy; Y_Hlx_db; Y_Odd_db; VH_dB	5
GA+ Grid SVR	150	0.20	Yam_Hlx; Anisotropy; Y_Hlx_db; Y_Odd_db; VH_dB	5

The comparisons between observed and predicted values coming from ALOS-2 PALSAR-2 data are presented through Fig.6 and Table VIII. The left column of Fig.6 shows scattered plots of observed and predicted forest AGB by using GA-SVR, GA+Default SVR, and GA+Grid SVR algorithm, respectively. It is clear from Fig.6 and Table VIII that the three algorithms performed worse on forest AGB estimation compering with the results of GF-3 data. The best performance acquired by

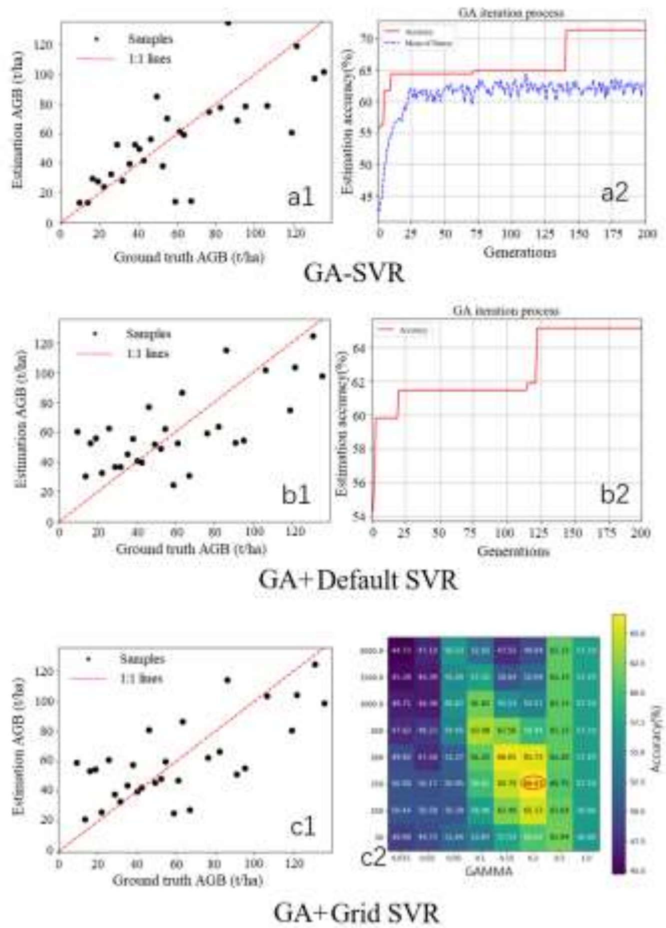

Fig.6. Biomass estimation results vs ground truth data (Results from ALOS-2 PALSAR-2). (a1) Iterative procedure of GA feature selection for GA-SVR algorithm; (a2) GA-SVR estimation results; (b1) GA iteration procedure for GA+Default SVR algorithm; (b2) GA+Default SVR estimation results; (c1) Grid model parameter searching procedure for GA+Grid SVR; (c1) GA+Grid SVR estimation results.

TABLE VIII
(ALOS-2 PALSAR-2) RESULTS COMPARISON BETWEEN GA-SVR, GA+DEFAULT SVR AND GA+GRID SVR

Methods	CVC (%)	RMSE (Mg/ha)	R^2
GA-SVR	71.41	17.35	0.55
GA+Default SVR	65.13	21.16	0.48
GA+Grid SVR	66.63	20.25	0.50

GA-SVR has the highest R^2 value of 0.55 and highest CVC value of 71.43%. The prediction results of GA+Grid SVR are lower than GA-SVR while better than GA+Default SVR with R^2 = 0.50 and CVC = 66.63%. The performance of three algorithms on ALOS-2 PALSAR-2 also confirmed the best performance of GA-SVR in forest AGB estimation. The iteration process in Fig.6 a2 shows the effectiveness of searching and convergence.

Fig.7 displays the spatial distribution of the estimated forest AGB by different estimation methods to the entire study area using GF-3 SAR data.

This article has been accepted for publication in a future issue of this journal, but has not been fully edited. Content may change prior to final publication. Citation information: DOI 10.1109/JSTARS.2021.3089151, IEEE Journal of Selected Topics in Applied Earth Observations and Remote Sensing

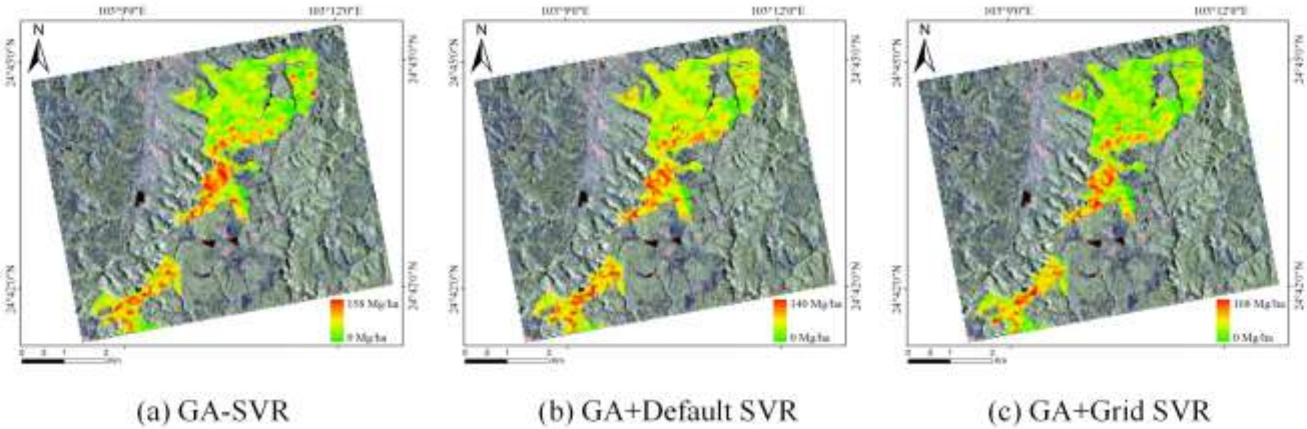

Fig.7. AGB maps showing the spatial application of GA-SVR、GA+Default SVR and GA+Grid SVR modeling approaches from GF-3 data

In Fig.7, AGB values higher than 200 Mg/ha are assumed to the overestimated the real biomass range in the study area and were therefore excluded. AGB values lower than 0 Mg/ha are unrealistic and were also assumed to be equal to 0 Mg/ha. The AGB spatial distribution maps show that forest AGB estimation results modeled by GA-SVR algorithm are more accurate both at lower and higher biomass level in the heterogeneous forest-covered areas. However, the AGB map modeled by GA+Default SVR seems more homogeneous and there are several over-estimations at lower biomass level, while few underestimations at higher level. The AGB spatial distribution of GA+Grid SVR is similar to GA-SVR but has higher upper range. Overall, one can states that AGB predicted by the GA-SVR algorithm achieved relatively good estimation result, which is balanced in both low and high biomass level and describes the filed AGB distribution scenario accurately.

VI. Discussion

Feature and model estimation parameter selection affects the forest AGB estimation. In this study, a GA was implemented for feature selection and model parameter optimization for SVR model simultaneously and then the results were applied in forest AGB estimation. The proposed algorithm is named as GA-SVR algorithm in this study. The performance of GA-SVR on forest AGB estimation was investigated and its performance was also compared with GA+Default SVR, in which algorithm GA was only implemented for feature selection, and GA+Grid SVR, in which algorithm GA was first used for feature selection and grid search was then used for model parameter estimation. The abilities of them for estimating forest AGB from C-band GF-3 and L-band ALOS-2 PALSAR-2 data were displayed and compared. The AGB estimation results from GF-3 and ALOS-2 PALSAR-2 data indicated that GA-SVR outperforms the other two algorithms. The similar results were demonstrated in remote sensing data classification using GA-SVM algorithm [16]. Previous studies demonstrated that AGB values within an accuracy requirement of 50 Mg/ha were accurate enough for the need of REDD+ [5]. All of the estimation bias of the three algorithms were less than 30 degradation and the role of conservation, sustainable management of forests and enhancement of forest carbon stocks in developing countries) [5]. All of the estimation bias of the three algorithms were less than 30 Mg/ha with both C-band and L-band SAR data. However, the GA-SVR was the most appropriate for the estimation of forest AGB since there is no obvious saturation effect in Fig.4 a1 and Fig.5 a1.

Forest AGB estimations using different SAR data were explored deeply in previous studies [3-5, 29-33]. A comparison of methods are necessary, however, as the diverse ecological environment effects on SAR data, it is difficult to compare various algorithms using different data, especially at the areas covered with different forest types or forest having different AGB levels [34-36]. A regression model with L-band HV backscatter got a highest RMSE of 23.61 Mg/ha at a restored mangroves area [29]. Artificial neural networks (ANN) models were reported superior to regress model in several studies [30], or achieved similar results [6,32]. In [30], the highest correlation coefficient between the biomass predicted by an ANN and that measured in the field was 0.829, while the value varied with the test site and the lowest value is 0.116. The RMSE values got in [5] and [32] were 22.03 Mg/ha and 48.2 Mg/ha, respectively. Other studies stated that SVR performed better than ANN [5,7], while ANN outperformed SVR for large-scale area. The study of [33] explored random forest kriging in modeling forest AGB and the RMSE value was 28.15 Mg/ha. GA was used for feature selection and then other estimation models with the GA selected feature were also applied in forest AGB estimation in recent years [4]. In this study, the performance of a proposed XGBR (extreme gradient boosting decision tree)-GA model was compared with that of SVR and other machine-learning models. The results confirmed the advantage of using GA for feature selection. The results of this study showed higher accuracy than several previous studies, especially applying in GF-3 data, but showed similar performance in the application of ALOS-2 PALSAR-2 data. It reveals the effectiveness of GA-SVR applied in forest AGB estimation although the influence of different perspectives like the satellite sensor, the structure of the forest and the environment factors.

Although several previous studies used GA feature selection

This article has been accepted for publication in a future issue of this journal, but has not been fully edited. Content may change prior to final publication. Citation information: DOI 10.1109/JSTARS.2021.3089151, IEEE Journal of Selected Topics in Applied Earth Observations and Remote Sensing

and estimation model parameter optimization separately, their results agreed the better performance of adding GA feature section or parameter optimization. Other studies which use GA for both feature selection and parameter optimization simultaneously, including this paper, revealed that performing feature selection and model parameter optimization simultaneously during the forest AGB estimation will improve the estimation accuracy and effectiveness.

The obvious difference between the selected SAR characters of GA-SVR for GF-3 and ALOS-2 PALSAR-2 is that the double bounce scattering characters were selected for GF-3 but not for ALOS-2, the HV characters were selected for ALOS-2 PALSAR-2, but not for GF-3. The phenomenon may result from the forest character of the test site. In the test site, the average forest above ground biomass is low and the trees in the sample plots are young and with low height (more of them are lower than 15m) and small average DBH (diameter at breast height, around 15 cm), C-band has the lower wave length than L- band, so more scattering from trunk like double bounce scattering, while for L-band, the lower height and small DBH make more depolarization scattering power. In previous studies, L- band shows better performance than C-band since it has a higher radar signal saturation limits, i.e. 20 tons/ha for C-band and 40 tons/ha for L-band [37]. However, in this study, C-band GF-3 SAR data shows better biomass estimation accuracies than L-band, it may result from the forest structure effects and low average biomass of the test site. Compared with the forest samples in literature [37], the forest density and the average biomass of our test site are lower. In our test site, the average height ranges from 5m～20m, the average biomass value is around 50 Mg/ha and the maximum biomass here is no more than 200 Mg/ha and the average canopy density is lower than 0.60 which may lead to more surface scattering at L-band than C-band. That means more backscattering to C-band came from forest than L-band. It may lead to better performance of C-band than L-band, however, it is need to be further explored in the future.

VII. Conclusion

The synchronous parameter optimization and feature selection processes of the SVR model are important technique for improving the accuracy of forest biomass estimation. 14 features and 2 groups of parameters were input the proposed GA-SVR algorithm to estimate forest biomass at the test site. The performance of the proposed GA-SVR algorithm was compared with the performance of the GA+ Default SVR and the performance of the GA+Grid SVR to determine the ability of each method to optimize the procedure of forest biomass estimation. The results showed that the estimation accuracy of the GA-SVR approach was greater than that of the GA+default SVR algorithm and the GA+Grid SVR algorithm. Although the GA+Grid SVR was commonly used for parameter optimization and feature selection processes of the SVR model, it optimized the features and parameters in two sequential steps, which neglected the synergy effects between two optimization procedures. By contrast, the GA-SVR algorithm optimized the parameters and features simultaneously and then provides better performance for forest biomass estimation. Although GA-SVR showed best performance among the three algorithms using both GF-3 and ALOS-2 PALSAR-2 data, it also showed obvious different estimation accuracy in different SAR data. Otherwise, the AGB level in this study was lower than 200 Mg/ha. Further investigations applying GA-SVR to other SAR data and forest type should be made and compared.

References

[1] Z. Liao, B. He, X. Bai and X. Quan, "Improving Forest Height Retrieval by Reducing the Ambiguity of Volume-Only Coherence Using Multi-Baseline PolInSAR Data," in *IEEE Transactions on Geoscience and Remote Sensing*, vol. 57, no. 11, pp. 8853-8866, Nov. 2019, doi: 10.1109/TGRS.2019.2923257.

[2] Z. Yang, Y. Shao, K. Li, Q. Liu, L. Liu, "An Improved Scheme for Rice Phenology Estimation Based on Time-Series Multispectral HJ-1A/B and Polarimetric RADARSAT-2 Data," in *Remote Sensing of Environment*, vol. 195, pp. 184-201, 2017, doi: 10.1016/j.rse.2017.04.016.

[3] D. Lu, Q. Chen, G. Wang, L. Liu, G. Li and E. Moran, "A Survey of Remote Sensing-Based Aboveground Biomass Estimation Methods in Forest Ecosystems," in *International Journal of Digital Earth*, vol. 9, pp. 63-105, 2016, doi: 10.1080/17538947.2014.990526

[4] T. D. Pham, N. Yokoya, J. Xia, H. N. Thang, and W. Takeuchi, " Comparison of Machine Learning Methods for Estimating Mangrove Above-Ground Biomass Using Multiple Source Remote Sensing Data in the Red River Delta Biosphere Reserve, Vietnam,".in *Remote Sensing*, vol. 12, no. 8, April 2020, doi: 10.3390/rs12081334

[5] S. Englhart, V. Keuck and F. Siegert, "Modeling Aboveground Biomass in Tropical Forests Using Multi-Frequency SAR Data—A Comparison of Methods," in IEEE Journal of Selected Topics in Applied Earth Observations and Remote Sensing, vol. 5, no. 1, pp. 298-306, Feb. 2012, doi: 10.1109/JSTARS.2011.2176720.

[6] Zhan H, Shi P, Chen C. Retrieval of oceanic chlorophyll concentration using support vector machines [J]. IEEE Transactions on Geoscience & Remote Sensing, 2003, 41(12):2947-2951.

[7] Camps-Valls G, Bruzzone L , Rojo-Alvarez J L , et al. Robust support vector regression for biophysical variable estimation from remotely sensed images[J]. IEEE Geoence and Remote Sensing Letters, 2006, 3(3):339-343.

[8] J. Monnet, J. Chanussot and F. Berger, "Support Vector Regression for the Estimation of Forest Stand Parameters Using Airborne Laser Scanning," in IEEE Geoscience and Remote Sensing Letters, vol. 8, no. 3, pp. 580-584, May 2011, doi: 10.1109/LGRS.2010.2094179.

[9] D. Whitley, "A genetic algorithm tutorial," in Statistics and Computing, vol.4, no.2, pp. 65-85, 1994, doi: 10.1007/BF00175354.

[10] G. A. Haddadi, M. R. Sahebi, and A. Mansourian, "Polarimetric SAR feature selection using a genetic algorithm, " in Canadian Journal of Remote Sensing, vol. 37, no. 1, pp. 27-36. 2011, doi: 10.5589/m11-013

[11] K. Xu, E. Chen, Z. Li, L. Zhao, W. Zhang and X. Wan, "The Wheat Biomass Estimation Based on Genetic Algorithm Feature Selection Method Using C-Band Polsar Data," *IGARSS 2019 - 2019 IEEE International Geoscience and Remote Sensing Symposium*, Yokohama, Japan, 2019, pp. 7231-7234, doi: 10.1109/IGARSS.2019.8898457.

[12] T. Olasupo, I. Alade, A. Bagudu, K. Sulaiman, S. Olatunji, T. Saleh, "Prediction of The Refractive Index of Haemoglobin Using the Hybrid GA-SVM Approach," in *Computers in Biology and Medicine*. vol. 98, pp. 85-92, Jul. 2018, doi: 10.1016/j.compbiomed.2018.04.024.

[13] K. Roushangar, A. Koosheh, "Evaluation of GA-SVR Method for Modeling Bed Load Transport in Gravel-Bed Rivers." in *Journal of Hydrology*.vol.527, pp.1142-4452,Aug.2015,doi:10.1016/j.jhydrol.2015.06.006.

[14] Z. Zhang, Y. Qin, L. Jia, J. Feng, M. An, L. Diao, "Metro Station Safety Status Prediction Based on GA-SVR," in *Proceedings of the 2015 International Conference on Electrical and Information Technologies for Rail Transportation*, vol. 378, pp. 57-69, Mar. 2016, doi: 10.1007/978-3-662-49370-0_7.

[15] A. Sanz-Garcia, J. Fernandez-Ceniceros, F. Antonanzas-Torres, A.V. Pernia-Espinoza, F.J. Martinez-de-Pison, "GA-PARSIMONY: A GA-SVR Approach with Feature Selection and Parameter Optimization to Obtain Parsimonious Solutions for Predicting Temperature Settings in a Continuous Annealing Furnace," in *Applied Soft Computing*, vo

l.35, pp. 13-28, Oct. 2015, doi: 10.1016/j.asoc.2015.06.012.

[16] C. Sukawattanavijit, J. Chen and H. Zhang, "GA-SVM Algorithm for Improving Land-Cover Classification Using SAR and Optical Remote Sensing Data," in *IEEE Geoscience and Remote Sensing Letters*, vol. 14, no. 3, pp. 284-288, March 2017, doi: 10.1109/LGRS.2016.2628406.

[17] A. J. Smola, B. Schölkopf, "A Tutorial on Support Vector Regression," in *Statistics and Computing*, vol. 14, pp. 199–222, 2004, doi: 10.1023/B:STCO.0000035301.49549.88

[18] H. Yu, S. Kim, "SVM Tutorial — Classification, Regression and Ranking," in *Rozenberg G., Bäck T., Kok J.N. (eds) Handbook of Natural Computing.* Springer, Berlin, Heidelberg. pp. 479-506, 2012, doi: 10.1007/978-3-540-92910-9_15.

[19] C. Huang, J. Zhang, W. Yang, X. Tang, A. J. Zhao, "Dynamics on forest carbon stock in Sichuan Province and Chongqing City," in *Acta Ecologica Siaica*, vol. 2S, no. 3, pp. 0966-0975, 2008. (in Chinese)

[20] X. Meng. *Forest mensuration*. Beijing: China Forestry Publishing House, 2006, pp.241-245. (in Chinese)

[21] H. L. G. Cassol, J. M. de B. Carreiras, E. C. Moraes, L. E. O. e C. de Aragão, C. V. de J. Silva, S. Quegan, and Y. E. Shimabukuro, "Retrieving Secondary Forest Aboveground Biomass from Polarimetric ALOS-2 PALSAR-2 Data in the Brazilian Amazon," in *Remote Sensing*, vol. 11, no. 1, pp. 59, Dec. 2018, doi: 10.3390/rs11010059

[22] F. Canisius, J. Shang, J. Liu, X. Huang, B. Ma, X. Jiao, X. Geng, J. M. Kovacs, D. Walters, "Tracking Crop Phenological Development Using Multi-Temporal Polarimetric Radarsat-2 Data," in Remote Sensing of Environment, vol. 210, pp. 508-518, Jun. 2018, doi: 10.1016/j.rse.2017.07.031.

[23] Y. Yamaguchi, T. Moriyama, M. Ishido and H. Yamada, "Four-component scattering model for polarimetric SAR image decomposition," in *IEEE Transactions on Geoscience and Remote Sensing*, vol. 43, no. 8, pp. 1699-1706, Aug. 2005, doi: 10.1109/TGRS.2005.852084.

[24] A. Freeman, "Fitting a Two-Component Scattering Model to Polarimetric SAR Data from Forests," in *IEEE Transactions on Geoscience and Remote Sensing*, vol. 45, no. 8, pp. 2583-2592, Aug. 2007, doi: 10.1109/TGRS.2007.897929.

[25] S. R. Cloude and E. Pottier, "A review of target decomposition theorems in radar polarimetry," in *IEEE Transactions on Geoscience and Remote Sensing*, vol. 34, no. 2, pp. 498-518, March 1996, doi: 10.1109/36.485127.

[26] A. Freeman S. L. Durden, "A three-component scattering model for polarimetric SAR data,"in *IEEE Transactions on Geoscience and Remote Sensing*,vol. 36, no. 3, pp. 963-973, May 1998, doi:10.1109/36.673687.

[27] G. Wiseman, H. McNairn, S. Homayouni and J. Shang, "RADARSAT-2 Polarimetric SAR Response to Crop Biomass for Agricultural Production Monitoring," in *IEEE Journal of Selected Topics in Applied Earth Observations and Remote Sensing*, vol. 7, no. 11, pp. 4461-4471, Nov. 2014, doi: 10.1109/JSTARS.2014.2322311.

[28] X. Wang, L.Fu and C.He, "Applying Support Vector Regression to Water Quality Modelling by Remote Sensing Data, " *in International Journal of Remote Sensing*, vol. 32, no. 23, December 2011, doi: 10.1080/01431161.2010.543183

[29] M. Nesha, Y. Hussin, L. Leeuwen and Y. Sulistioadi, "Modeling and mapping aboveground biomass of the restored mangroves using ALOS-2 PALSAR-2 in East Kalimantan, Indonesia," in *International Journal of Applied Earth Observation and Geoinformation*, vol.91, no. 102158, Sep. 2020, doi: 10.1016/j.jag.2020.102158.

[30] G. M. Foody, D. S. Boyd and M. E. J. Cutler, "Predictive relations of tropical forest biomass from Landsat TM data and their transferability between regions," in *Remote Sensing of Environment*, vol. 85, no. 4, pp. 463-474, Jun. 2003, doi: 10.1016/S0034-4257(03)00039-7.

[31] A. Wijaya, V.Liesenberg and R. Gloaguen, "Retrieval of forest attributes in complex successional forests of Central Indonesia: Modeling and estimation of bitemporal data,"in *Forest Ecology and Management*, vol. 259 ,no.12,pp .2315-2326,May .2010,doi:10.1016/j.foreco.2010.03.004.

[32] P. Muukkonen, J. Heiskanen, "Estimating biomass for boreal forests using ASTER satellite data combined with standwise forest inventory data," in *Remote Sensing of Environment*, vol. 99, no. 4, pp. 434-447, Dec. 2005, doi: 10.1016/j.rse.2005.09.011.

[33] L. Chen, Y. Wang, C. Ren, B. Zhang and Z. Wang, "Assessment of multi-wavelength SAR and multispectral instrument data for forest aboveground biomass mapping using random forest kriging," in *Forest Ecology and Management*, vol. 447, pp. 12-25, Sep. 2019, doi: 10.1016/j.foreco.2019.05.057.

[34] D. Lu, "The potential and challenge of remote sensing-based biomass estimation," in *International Journal of Remote Sensing*, vol. 27, no. 7, pp. 1297-1328, 2006, doi: 10.1080/01431160500486732

[35] S. Saatchi, M. Marlier, R. L. Chazdon, D. B. Clark and A. E. Russell, "Impact of spatial variability of tropical forest structure on radar estimation of aboveground biomass," in *Remote Sensing of Environment*, Vol. 115, no. 11, pp. 2836-2849, Nov. 2011, doi: 10.1016/j.rse.2010.07.015.

[36] Y. Ji, J. Huang, Y. Ju, S. Guo, C. Yue. "Forest structure dependency analysis of L-band SAR backscatter," in *PeerJ*, vol.8， no. e10055, Sep. 2020, doi: 10.7717/peerj.10055.

[37] Imhoff, M. L. Radar backscatter and biomass saturation: ramifications for global biomass inventory [J]. Geoscience and Remote Sensing, IEEE Transactions on, 1995.

Yongjie Ji received the MA.Sc degree in Cartography and Geographical Information System from Southwest Forestry University, China, in 2013. He is currently pursuing the Ph.D. degree in forestry remote sensing at Southwest Forestry University, College Station, Kunming, China.

From 2013 to present, he was a Research Assistant with School of Geography and Ecotourism, Southwest Forestry University, Kunming. His research interest focus on forest canopy height and forest biomass estimation using PolInSAR and SAR data. He has published more than 20 papers in referred journals or presentations in international conferences and symposia.

Kunpeng Xu received the M.S. degree in cartography and geographical information system from Inner Mongolia Normal University, Hohhot, China, in 2015. He is currently working toward the Ph.D. degree in forest management at the Institute of Forest Resources Information Technique, Chinese Academy of Forestry, Beijing, China.
His research interests include remote sensing image processing, polarimetric/interferometric SAR application, and machine learning.

Peng Zeng received the B.S. in geography science from Zhangjiakou University, China, in 2018.
He is currently a post graduate with Southwest Forestry University, China. His main learn and research field focus on radar remote sensing applied in forest resources.

This article has been accepted for publication in a future issue of this journal, but has not been fully edited. Content may change prior to final publication. Citation information: DOI 10.1109/JSTARS.2021.3089151, IEEE Journal of Selected Topics in Applied Earth Observations and Remote Sensing

Wangfei Zhang received both the B.S. degree in Land Resource Management and the M.S. degree in Cartography and Geography Information System from Wuhan University, Wuhan, China , in 2001 and 2004, respectively, and the Ph.D. degree in Geophysical Prospecting and Information Technology from Kunming University of Science and Technology, Kunming, China, in 2011.

She was a Post-Doctoral Researcher at Institute of Forest Resources Information Technique, Chinese Academy of Forestry, Beijing, China. From 2014 to 2015, She worked as a visiting scholar at remote sensing group in University of Victoria and Pacific Forestry Centre, Victoria, Canada. In 2004, she joined the College of Forestry, Southwest Forestry University, Kunming, China, where she is a doctoral supervisor and professor currently. She has co-authored more than 50 papers in referred journals or presentations in international conferences and symposia. Her research interests include microwave remote sensing for inversion of crop and forest biophysical parameters, polarimetric and interferometric techniques and numerical models of vegetation microwave scattering problems.